

An Improved Algorithm for the Three-Fluid-Phase VLE Flash Calculation

Humberto Hinojosa-Gómez and Jorge Solares-Ramírez

Centro de Innovación en Hidrocarburos-Grupo SSC Oil & Gas Division, Escuadrón 201 8, San Miguel de Allende, 37748 Guanajuato, México

Enrique R. Bazúa-Rueda

Dept. de Ingeniería Química, Facultad de Química, Universidad Nacional Autónoma de México, Av. Universidad 3000, 04510 México D.F., México

DOI 10.1002/aic.14946

Published online August 7, 2015 in Wiley Online Library (wileyonlinelibrary.com)

The VLE flash is important in water and hydrocarbons mixtures, hydrocarbon and CO₂ rich mixtures, and hydrocarbon methane rich mixtures that are encountered in reservoir performance and recovery studies. A robust VLE flash algorithm is proposed. The equilibrium and mass balance equations are solved as a constrained minimization problem. An inverse barrier function is used to handle the inequality constraints to solve for the phase fractions. It warrants always arriving to the solution. The challenging cases analyzed showed that the initialization procedure proposed, together with successive substitution iteration in the outer loop, is a good method for a stable VLE flash algorithm, even near critical points. Whenever the result is in the region outside the three-phase physical domain, the solution suggests that the system has fewer phases. In one of the cases analyzed, a region with three liquid phases was encountered and the algorithm found two different solutions with positive phase fractions. © 2015 American Institute of Chemical Engineers *AICHE J*, 61: 3081–3093, 2015

Keywords: computational chemistry (kinetics/thermo), phase diagrams, phase equilibrium, vapor-liquid-liquid equilibrium

Introduction

The three-fluid-phase Vapor-Liquid-Liquid Equilibrium (VLE) flash calculation is important in a variety of problems relevant in chemical engineering. In many processes, three fluid phases may be present when the liquid phase splits into two liquids, consequently, the phase equilibrium calculation has to recognize the regions where one (V or L), two (VL or LL), or three fluid phases (VLL) are present. Such is the case in water and hydrocarbons mixtures, hydrocarbon and CO₂ rich mixtures and hydrocarbon CH₄ rich mixtures found in reservoir performance and recovery studies.

The fluid phase equilibrium problem is formulated as follows: given a mixture whose global composition is known, the compositions and amounts of fluid phases present in equilibrium at a given temperature and pressure, must be determined. The phase with the lowest density is labeled as vapor, the remaining ones as liquids. Thermodynamic models that represent the properties of the fluid phases must be provided. In the event that the equilibrium problem solution is required to cover the complete phase space, including the critical region, an equation of state (EOS)-based model is adopted.

Over the past three decades, many multiphase algorithms have been proposed to solve the highly nonlinear equilibrium problem. The problem has been formulated in two broad cate-

gories: (1) equi-fugacity methods (EFM), and 2) Gibbs free energy minimization methods (GMM). In the EFM method, the formulation pursues the equality of fugacity and the mass balance equations. The EFM method solves for the phase fractions in an inner loop and the phase compositions are updated in the outer loop. The inner loop can be formulated as a minimization problem or as an equation-solving problem. The GMM method is formulated as a Gibbs energy minimization subject to mass balance constraints. For the two approaches, there are several algorithms recently developed that provide solutions to difficult equilibrium problems. Apparently, both approaches are capable to find the solution even with difficult problems, and the selection of a specific approach is a matter of preferences.

Recent works on the EFM have placed special attention to the solution of the Rachford–Rice (RR) equations to guaranty robustness and stability of the solution. Implementing the negative flash strategy is necessary for a robust algorithm (Whitson and Michelsen¹). In this approach, a major problem found is that classical Newton's method fails to converge in difficult regions like near critical points and phase boundaries. Proposals to overcome this deficiency are the formulation of Iranshahr et al.² and Leibovici and Neoschil³ that uses the Newton's method with a relaxation parameter, of Haugen et al.⁴ and Li and Firoozabadi^{5,6} using the two-dimensional bisection method to obtain initial guesses of phase fractions and then solving the RR equations by Newton's Method, of Okuno et al.⁷ that uses a line search along the Newton's

Correspondence concerning this article should be addressed to E. Bazua-Rueda at erbr@unam.mx.

direction and the formulation of Yan and Stenby⁸ that analyzes the use of higher order methods. To solve the RR equations, Michelsen⁹ proposed the minimization of a function whose derivatives are the RR equations and Leibovici and Nichita¹⁰ added the negative flash concept to Michelsen's formulation with good results.

Conversely, works on the GMM approach are the formulation of Lucia et al.¹¹ that uses the full space SQP algorithm, of Bausa and Marquardt¹² that employs homotopy continuation, of Saber and Shaw¹³ that uses the so-called DIRECT method, of Jalali et al.¹⁴ that applies homotopy continuation in the complex domain, of Nichita and Gomez¹⁵ that uses tunneling global optimization and of Petitfrere and Nichita¹⁶ on the trust region method.

To find the correct number of phases present for a given problem, the strategies proposed have been along the following lines: (1) start with a stability analysis to see if the mixture splits in two phases, then solve the two phase flash, follow with a stability analysis to see if the system splits in three phases, and finally, solve the VLLE flash^{4-6,11-13,16,17}; (2) start with the three-phase VLLE flash,² if the solution is in the VLL region, accept the solution, otherwise, perform the corresponding two phase flash (VL or LL).

As a starting point for any VLLE flash algorithm is the initialization procedure. First, there is the need to provide initial estimates of compositions and fractions of the phases present. Poor estimates can lead to not finding the correct solution or not finding a solution at all. Several algorithms perform first, as pointed out previously, a one-phase stability analysis to provide initial estimates for the two-phase flash problem, then use the results from two-phase split calculation and, if an instability is found with a two-phase stability analysis, a three-phase flash is solved.^{4-6,11-13,16-18} Another option is to start directly with estimates from ideal Wilson K's for vapor and one liquid phases and the second liquid phase with the key component concept.^{19,20} This option is commonly used in VLE or LLE flash calculations but it seems to be not used with frequency in VLLE flash calculations. If one is performing repeated flash calculations, then the solution of the previous flash calculation can be adopted as starting point for the next calculation.

The main difference in the procedures outlined in previous works lies in the decision of when to calculate the VLLE flash, along with the initialization procedure. In any case, one needs a VLLE flash algorithm capable of finding a solution whenever it exists.

Based on the major findings of previous works, we present a VLLE flash algorithm that takes into account the following aspects:

1. The VLLE flash algorithm has to be capable of finding the solution in the feasible VLLE region, including the negative flash zone. It has to be robust and efficient, even in hard to find situations like close to critical points. It has to exhibit continuity along the VLL phase boundaries.

2. The VLLE flash has to converge starting with a general simple initialization.

3. The phase distribution is calculated at fixed equilibrium constants in an inner loop followed by the update of component mole fractions in an outer loop.

4. As starting point, we use the modification of Michelsen's function⁹ proposed by Leibovici and Nichita,¹⁰ along with the negative flash approach.

5. The minimization of the modified Michelsen's function is performed with the aid of an inverse barrier function to

handle the inequality constraints to solve for the phase fractions.

6. The solution may suggest the number of phases for a given global composition of a mixture.

7. For illustration purposes, the Peng–Robinson²¹ (PR) EOS is the thermodynamic model that is adopted to represent the properties of the fluid phases.

Problem Formulation

The VLLE flash is formulated as: given a mixture of known global composition, the amounts and compositions of the vapor and two liquid phases present in equilibrium at a given temperature and pressure, must be determined. In the EFM approach, the system of equations that must be solved are the usual equilibrium and material balance relations for each component in the mixture

1. Equilibrium equations

$$f_i^V = f_i^{L_1} = f_i^{L_2} \quad i = 1, \dots, n \quad (1)$$

In terms of equilibrium constants, they are expressed as

$$K_{1i} = \frac{y_i}{x_i} = \frac{\phi_i^{L_1}}{\phi_i^V} \quad K_{2i} = \frac{w_i}{x_i} = \frac{\phi_i^{L_2}}{\phi_i^V} \quad i = 1, \dots, n \quad (2)$$

The fugacity coefficients for the three fluid phases are calculated with the PR EOS and are functions of temperature, pressure, and phase composition.

2. Material balance equations

$$z_i = \beta_1 y_i + \beta_2 w_i + (1 - \beta_1 - \beta_2) x_i \quad i = 1, \dots, n \quad (3)$$

The phase fractions are

$$\frac{V}{F} = \beta_1 \quad \frac{L_2}{F} = \beta_2 \quad \frac{L_1}{F} = (1 - \beta_1 - \beta_2) \quad (4)$$

Equations 2 and 3 are combined in the usual manner to give the equations for the phase compositions in terms of phase fractions and equilibrium constants

$$x_i = \frac{z_i}{1 + \beta_1(K_{1i} - 1) + \beta_2(K_{2i} - 1)} \quad i = 1, \dots, n \quad (5)$$

$$y_i = \frac{z_i K_{1i}}{1 + \beta_1(K_{1i} - 1) + \beta_2(K_{2i} - 1)} \quad i = 1, \dots, n \quad (6)$$

$$w_i = \frac{z_i K_{2i}}{1 + \beta_1(K_{1i} - 1) + \beta_2(K_{2i} - 1)} \quad i = 1, \dots, n \quad (7)$$

The system formed by Eqs. 2 and 5–7, together with the restriction that the phase mole fractions have to add to unity should be recursively solved. The unknowns are the phase fractions β_1 , β_2 , and the phase component mole fractions x_i , y_i , w_i , $i = 1, \dots, n$. The number of unknowns is: 2 phase fractions (the third one adds to unity) and $3(n - 1)$ phase component mole fractions (the remaining one adds to unity for each phase.)

In the EFM approach, it is usual to combine Eqs. 5–7 to give the RR equations

$$\text{RR}_{yx} = \sum_{i=1}^n \frac{z_i(K_{1i} - 1)}{1 + \beta_1(K_{1i} - 1) + \beta_2(K_{2i} - 1)} = 0 \quad (8)$$

$$\text{RR}_{wx} = \sum_{i=1}^n \frac{z_i(K_{2i} - 1)}{1 + \beta_1(K_{1i} - 1) + \beta_2(K_{2i} - 1)} = 0 \quad (9)$$

The general EFM strategy is to solve Eqs. 8 and 9 for β_1 and β_2 for a given set of equilibrium constants K_{1i} and K_{2i} for

$i = 1, \dots, n$ in an inner loop. Then, in an outer loop, a new estimate of phase component mole fractions is calculated with Eqs. 5–7 and the equilibrium constants updated through Eq. 2 with fugacity coefficients from the EOS. This procedure is called successive substitution iteration (SSI). The difficulty in finding a solution is highly related to the phase compositions dependency of the fugacity coefficients. This is the case when the critical points are approached and when the liquid phase shows nonidealities that can cause a phase split.

As it can be seen in the previous work mentioned above, many strategies have been proposed to solve the RR equations in the inner loop.^{2–10} In the present work, we adopted the modification of Leibovici and Nichita¹⁰ to Michelsen's⁹ formulation as a constrained minimization problem. We introduced an inverse barrier function²² to construct a composite function that combines the objective function and the inequality constrained functions in such a way as to introduce a barrier along the constrained boundary.

The formulation is as follows.

Following Leibovici and Nichita,¹⁰ given a set of equilibrium constants K_{1i} and K_{2i} for $i = 1, \dots, n$, find the phase fractions $\theta = (\beta_1, \beta_2)$ that minimizes the objective function

$$Q(\theta) = 1 - \frac{1}{2} \sum_{i=1}^n z_i \ln [1 + \beta_1 (K_{1i} - 1) + \beta_2 (K_{2i} - 1)]^2 \quad (10)$$

Subject to the inequality constraints

$$E_i = 1 + \beta_1 (K_{1i} - 1) + \beta_2 (K_{2i} - 1) > 0 \quad i = 1, \dots, n \quad (11)$$

The inequality constraints warrant that the component mole fractions in all phases are positive. Equation 11 defines the feasible region. The phase fractions are allowed to take values in the feasible region even if a negative value for one phase fraction is found. A solution is sought in all the domain of the feasible region.

The inequality constraints are combined with the objective function through the inverse barrier function

$$B(\theta, r) = Q(\theta) + r \sum_{i=1}^n \frac{1}{E_i} \quad (12)$$

The problem is now to solve for the phase fractions β_1, β_2 that minimize the augmented function $B(\theta, r)$. The barrier parameter has to be chosen so that the trial values of the phase fractions remain in the feasible region. It must adopt a non-negative value. In subsequent iterations it has to diminish and become zero as the solution is approached. If the barrier parameter is properly chosen, an unconstrained search technique can be implemented.

The minimum of the augmented function is found when the derivatives of the augmented function are equal to zero

$$B_{yx} = \frac{\partial B}{\partial \beta_1} = - \sum_{i=1}^n \frac{z_i (K_{1i} - 1)}{1 + \beta_1 (K_{1i} - 1) + \beta_2 (K_{2i} - 1)} - r \sum_{i=1}^n \frac{(K_{1i} - 1)}{[1 + \beta_1 (K_{1i} - 1) + \beta_2 (K_{2i} - 1)]^2} = 0 \quad (13)$$

$$B_{wx} = \frac{\partial B}{\partial \beta_2} = - \sum_{i=1}^n \frac{z_i (K_{2i} - 1)}{1 + \beta_1 (K_{1i} - 1) + \beta_2 (K_{2i} - 1)} - r \sum_{i=1}^n \frac{(K_{2i} - 1)}{[1 + \beta_1 (K_{1i} - 1) + \beta_2 (K_{2i} - 1)]^2} = 0 \quad (14)$$

It should be noted that the usual RR equations are fulfilled if the barrier parameter is equal to zero. The problem is trans-

formed to find a solution of Eqs. 13 and 14 for the phase fractions β_1, β_2 . To do so, we have selected a Newton's search method. The necessary derivatives for the gradient are

$$\frac{\partial B_{yx}}{\partial \beta_1} = \sum_{i=1}^n \frac{z_i (K_{1i} - 1)^2}{[1 + \beta_1 (K_{1i} - 1) + \beta_2 (K_{2i} - 1)]^2} + 2r \sum_{i=1}^n \frac{(K_{1i} - 1)^2}{[1 + \beta_1 (K_{1i} - 1) + \beta_2 (K_{2i} - 1)]^3}$$

$$\frac{\partial B_{wx}}{\partial \beta_2} = \sum_{i=1}^n \frac{z_i (K_{2i} - 1)^2}{[1 + \beta_1 (K_{1i} - 1) + \beta_2 (K_{2i} - 1)]^2} + 2r \sum_{i=1}^n \frac{(K_{2i} - 1)^2}{[1 + \beta_1 (K_{1i} - 1) + \beta_2 (K_{2i} - 1)]^3}$$

$$\frac{\partial B_{yx}}{\partial \beta_2} = \frac{\partial B_{wx}}{\partial \beta_1} = \sum_{i=1}^n \frac{z_i (K_{1i} - 1) (K_{2i} - 1)}{[1 + \beta_1 (K_{1i} - 1) + \beta_2 (K_{2i} - 1)]^2} + 2r \sum_{i=1}^n \frac{(K_{1i} - 1) (K_{2i} - 1)}{[1 + \beta_1 (K_{1i} - 1) + \beta_2 (K_{2i} - 1)]^3}$$

If we denote the current trial value for the phase fractions as $(\beta_1)_0$ and $(\beta_2)_0$, the updated values are obtained with

$$\beta_1 = (\beta_1)_0 + \frac{(-S_1 - r S_6) (S_4 + 2r S_9) - (-S_2 - r S_7) (S_5 + 2r S_{10})}{(S_5 + 2r S_{10})^2 - (S_4 + 2r S_9) (S_3 + 2r S_8)} \quad (15)$$

$$\beta_2 = (\beta_2)_0 + \frac{(-S_2 - r S_7) (S_3 + 2r S_8) - (-S_1 - r S_6) (S_5 + 2r S_{10})}{(S_5 + 2r S_{10})^2 - (S_4 + 2r S_9) (S_3 + 2r S_8)} \quad (16)$$

Where the summations S_1 to S_{10} are given by

$$\begin{aligned} S_1 &= \sum_{i=1}^n \frac{z_i (K_{1i} - 1)}{1 + \beta_1 (K_{1i} - 1) + \beta_2 (K_{2i} - 1)} \\ S_6 &= \sum_{i=1}^n \frac{(K_{1i} - 1)}{[1 + \beta_1 (K_{1i} - 1) + \beta_2 (K_{2i} - 1)]^2} \\ S_2 &= \sum_{i=1}^n \frac{z_i (K_{2i} - 1)}{1 + \beta_1 (K_{1i} - 1) + \beta_2 (K_{2i} - 1)} \\ S_7 &= \sum_{i=1}^n \frac{(K_{2i} - 1)}{[1 + \beta_1 (K_{1i} - 1) + \beta_2 (K_{2i} - 1)]^2} \\ S_3 &= \sum_{i=1}^n \frac{z_i (K_{1i} - 1)^2}{[1 + \beta_1 (K_{1i} - 1) + \beta_2 (K_{2i} - 1)]^2} \\ S_8 &= \sum_{i=1}^n \frac{(K_{1i} - 1)^2}{[1 + \beta_1 (K_{1i} - 1) + \beta_2 (K_{2i} - 1)]^3} \\ S_4 &= \sum_{i=1}^n \frac{z_i (K_{2i} - 1)^2}{[1 + \beta_1 (K_{1i} - 1) + \beta_2 (K_{2i} - 1)]^2} \\ S_9 &= \sum_{i=1}^n \frac{(K_{2i} - 1)^2}{[1 + \beta_1 (K_{1i} - 1) + \beta_2 (K_{2i} - 1)]^3} \\ S_5 &= \sum_{i=1}^n \frac{z_i (K_{1i} - 1) (K_{2i} - 1)}{[1 + \beta_1 (K_{1i} - 1) + \beta_2 (K_{2i} - 1)]^2} \\ S_{10} &= \sum_{i=1}^n \frac{(K_{1i} - 1) (K_{2i} - 1)}{[1 + \beta_1 (K_{1i} - 1) + \beta_2 (K_{2i} - 1)]^3} \end{aligned}$$

To find an appropriate value for the barrier parameter r , we calculate the minimum value that warrant the inequalities, Eq.

11, are always meet. Substituting Eqs. 15 and 16 into Eq. 11, the following expression is obtained

$$E_i = (E_i)_0 + \frac{a_i + b_i r + c_i r^2}{A + B r + C r^2} \quad i = 1, \dots, n \quad (17)$$

Where

$$(E_i)_0 = 1 + (\beta_1)_0 (K_{1i} - 1) + (\beta_2)_0 (K_{2i} - 1)$$

$$a_i = (-S_1 S_4 + S_2 S_5) (K_{1i} - 1) + (-S_2 S_3 + S_1 S_5) (K_{2i} - 1)$$

$$b_i = (-2 S_1 S_9 + 2 S_2 S_{10} - S_4 S_6 + S_5 S_7) (K_{1i} - 1) + (-2 S_2 S_8 + 2 S_1 S_{10} - S_3 S_7 + S_5 S_6) (K_{2i} - 1)$$

$$c_i = (-2 S_6 S_9 + 2 S_7 S_{10}) (K_{1i} - 1) + (-2 S_7 S_8 + 2 S_6 S_{10}) (K_{2i} - 1)$$

$$A = S_5^2 - S_3 S_4$$

$$B = 4 S_5 S_{10} - 2 S_4 S_8 - 2 S_3 S_9$$

$$C = 4 (S_{10}^2 - S_8 S_9)$$

The equations $E_i = 0$ are quadratic with respect to the barrier parameter r and are solved for r for each component in the mixture. The barrier parameter r , substituted in Eqs. 15 and 16 to update the phase fractions is chosen as 1.5 times the maximum real root encountered in solving Eq. 17 equated to zero for all components. If a negative value is found, then r is set equal to zero. In this case, the algorithm is equivalent to a Newton's second-order convergence because imposing a barrier was not necessary to ensure the convergence. The barrier parameter has to be zero when the convergence is reached.

The previous formulation warrants finding a solution whenever a solution exists. If, for the given set of equilibrium constants a solution does not exist, the iterations proceed to negative values of increasing magnitude for one of the phases.

Solution Procedure

The algorithm proposed in this work for the VLLE flash problem is as follows:

1. Initial estimates of the phase fractions are set to $\beta_1 = 0.3$ and $\beta_2 = 0.3$.
2. Initial estimates of the phase compositions are given by

$$\text{For the vapor phase } y_i = z_i K_i^W \quad i = 1, \dots, n$$

$$\text{For the first liquid phase } x_i = z_i / K_i^W \quad i = 1, \dots, n$$

Where the K_i^W is the usual Wilson's VL equilibrium constant

$$K_i^W = \frac{p_{ci}}{p} \exp\left(5.373(1 + \omega_i) \left(1 - \frac{T_{ci}}{T}\right)\right) \quad i = 1, \dots, n$$

For the second liquid phase, we choose it to be almost a pure component.^{19,20} The proposed mole fraction value for the key component of Li and Firoozabadi⁵ is 0.90. However, we tested several values (0.9, 0.95, and 0.98) and adopted a mole fraction equal to 0.98 for the key component as it gave the most consistent results for the systems studied in this work. The remaining 0.02 is evenly distributed among the rest of the components. In principle, all components are chosen to be key components.

3. Calculate the fugacity coefficients for each component in every phase using the EOS. For the first iterations, the algorithm of Mathias et al.²³ is implemented to avoid trivial solutions. Then, the equilibrium constants are calculated with Eq. 2.

4. Solve the inner loop to find the phase fractions $\theta = (\beta_1, \beta_2)$ for the equilibrium constants calculated in Step 3 with

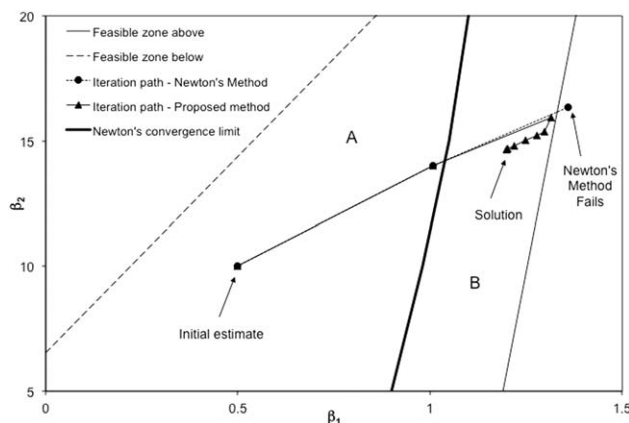


Figure 1. Iteration path for Example 4 from Okuno et al.⁷ Newton's iterations (dot) and proposed method (triangles).

Feasible zone above solid line and below dashed line. The gross solid line divides the Sector B (Newton's method converges) and Sector A (Newton's method fails).

the augmented barrier function formulation presented in this work, as explained earlier. The phase fractions are allowed to take values in the feasible region even if a negative phase is encountered. Continue the iterations until the residual of the barrier function Eqs. 13 and 14 are lower than a specified tolerance. If the iterations proceed to negative values of increasing magnitude for one of the phases the iteration is stopped and a warning is issued stating that for the conditions given either (a) there is not a solution of the RR equations for the given set of equilibrium constants, (b) the solution is very close to the limit of the feasible region, or (c) the problem is very close to a critical point.

5. Update the phase component mole fraction with Eqs. 5–7. Normalize so that they add to unity.

6. Check for convergence and go back to Step 3 for the next iteration if needed. This is the SSI in the outer loop.

Results

Haugen et al.⁴ stress the importance of finding the solution in the inner loop where a solution of the three-phase flash is sought for a given set of equilibrium constants. This is a necessary requisite for a stable VLLE flash algorithm. To illustrate the convergence properties of the algorithm proposed in this work for the inner loop, in Figures 1 and 2 we present results of Examples 3 and 4 given by Okuno et al.⁷ in their Table 2. The feasible zone is located in the usual manner delimited by the lines drawn where the inequality constraints given by Eq. 11 are set equal to zero. The feasible zone is divided into two sectors depending on the convergence properties of a Newton's algorithm. If the initial estimates of the phase fractions fall in Sector B, the Newton's algorithm will converge, but if it fall in Sector A the Newton algorithm will not converge because in one of the iterations the phase fractions will adopt values outside the feasible zone. The solution to the flash problem always lies in the Newton's convergence sector. For these examples, the Newton's convergence Sector B is very narrow and therefore can be used to prove the convergence characteristics of the inner loop algorithms. As it is shown in Figure 1, the barrier method proposed in this work is capable during all iterations to maintain the successive values of phase fractions

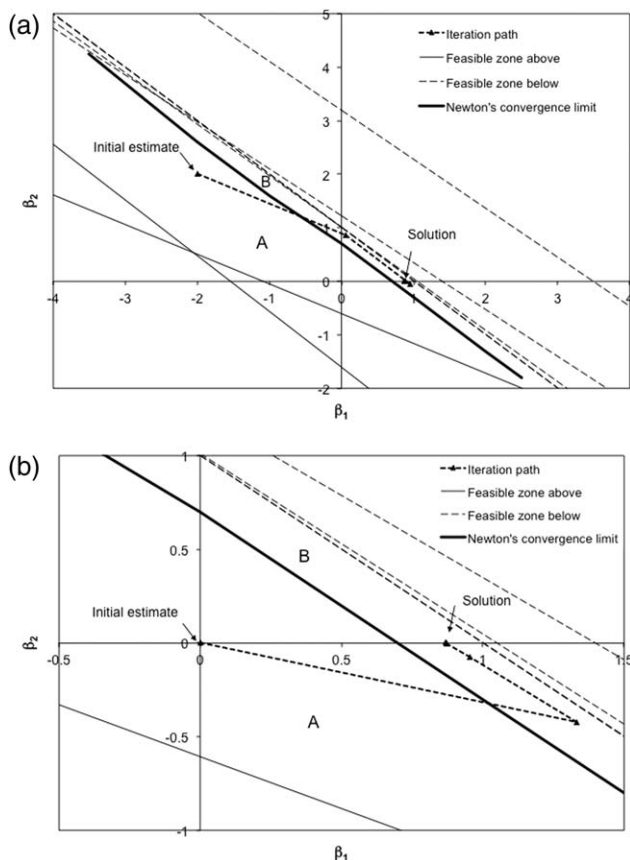


Figure 2. Iteration path for Example 3 from Okuno et al.⁷ for two initial estimates.

Newton's iterations (dot) and proposed method (triangles). Feasible zone above solid line and below dashed lines. The gross solid line divides the Sector B (Newton's method converges) and Sector A (Newton's method fails).

in the feasible zone. This is done by using a positive value of the barrier parameter. In this particular example, a positive value of the barrier parameter was needed in the second iteration. As shown in Figure 2 for Example 3, the proposed algorithm can find a solution starting with different initial estimates. It takes a few iterations to drive the solution to the Newton's sector where convergence is located.

For a multicomponent system of given global composition at a specified temperature and pressure, the solution of the three-phase flash VLE problem can fall into one of the following situations: (a) convergence to the physical feasible solution for which all phase fractions are positive, (b) convergence in the negative flash region where one of the phase fractions is negative, or (c) there is not solution to the VLE problem. The last situation arises when the stated conditions for the VLE flash problem are beyond the asymptotes, as discussed by Leibovici and Nichita.¹⁰

To test the proposed algorithm in this work, we systematically analyzed five challenging problems addressed by Haugen et al.⁴ and Li and Firoozabadi⁵ (CO₂ injection for Oil B, Malhamar Reservoir Oil, Malhamar Separator Oil, Bob Slaughter Block Oil, and North Ward Estes Oil). For the Bob Slaughter Block Oil and North Ward Estes Oil, we injected pure CO₂, as it is done with the other three systems. Haugen et al.⁴ and Li and Firoozabadi⁵ injected impure CO₂ (95% CO₂ + 5% CH₄) for these systems, so our results are not quite comparable with

Haugen et al.⁴ and Li and Firoozabadi⁵ results for these two systems. We used the PR EOS for the fugacity coefficients calculations in all phases. The compositions, critical properties, acentric factors, and nonzero binary interaction coefficients were taken from the Tables 4–8 in Li and Firoozabadi.⁵

In Figures 3–7, we present the phase diagrams for the systems studied. All the phase diagrams were constructed with the VLE algorithm proposed in this work. The results we obtained compare well with the results of Haugen et al.⁴ and Li and Firoozabadi.⁵ Note that for the North Ward Estes Oil system there is not a CO₂-rich bicritical point in our calculations as compared with Haugen et al.⁴ results due to the difference in composition of the CO₂ injected.

At a specified pressure and CO₂ mole fraction, the VLE flash was solved with the algorithm outlined in Solution Procedure Section, always starting from the stand-alone initial estimate. The negative-flash algorithm always converged to a solution if the specified conditions fall inside the VLE flash convergence limits. Whenever a phase boundary line is crossed, a new phase appears or disappears depending on the direction that the line is crossed. Then, along the phase boundary line, the phase fraction of one of the phases in equilibrium is equal to zero. To locate the points in the phase diagrams presented in this work, an interpolation of the VLE negative-flash solutions was performed. The enlargements around the bicritical points show a retrograde behavior not reported by

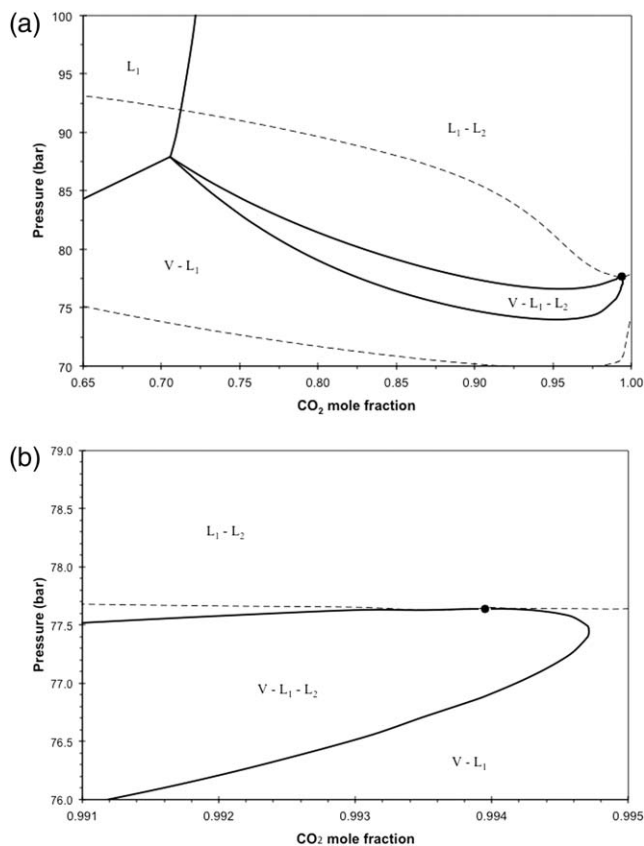


Figure 3. The phase diagram for CO₂ mixing with Oil B at 307.6 K showing the phase regions.

V, L₁, L₂ are the vapor, CO₂-lean, and CO₂-rich liquid phases. The solid lines are the phase boundaries and the dashed lines are the VLE flash convergence limit. The solid circle represents the bicritical point. (a) Complete phase diagram and (b) enlargement around the CO₂-rich bicritical point.

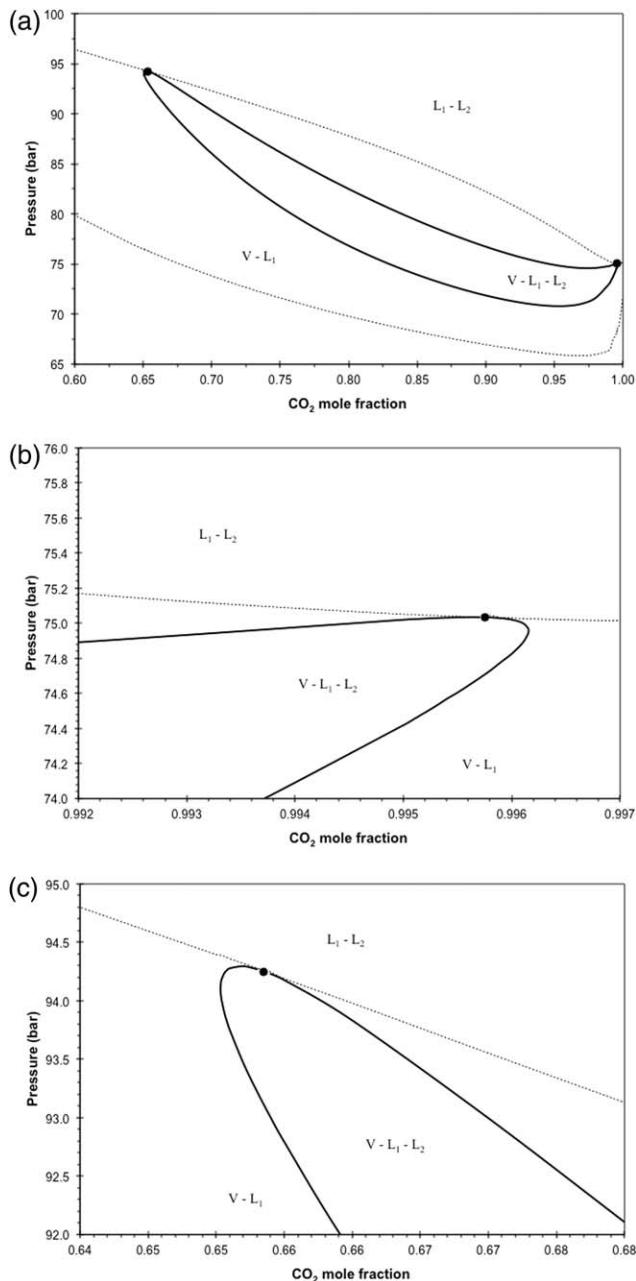


Figure 4. The phase diagram for CO₂ mixing with Malhamar Reservoir Oil at 305.35 K showing the phase regions.

V , L_1 , L_2 are the vapor, CO₂-lean, and CO₂-rich liquid phases. The solid lines are the phase boundaries and the dashed lines are the VLLE flash convergence limit. The solid circles represent the bicritical points. (a) Complete phase diagram, (b) enlargement around the CO₂-rich bicritical point, and (c) enlargement around the CO₂-lean bicritical point.

previous works on the same systems. The convergence limits lines drawn on the phase diagrams correspond to solutions of the VLLE negative-flash for which a phase fraction for one of the phases is equal to +5 or -5. With these limits, we make sure to be close to the asymptotes. The VLLE region enclosed by the convergence limits cover a much wider area than the physically feasible three phase VLLE region enclosed by the phase boundaries. As the convergence limit is approached, the difference in composition of two of the phases becomes very

small. The two phases with this behavior are the ones with the phase fraction large in magnitude, one positive and the other one negative. Therefore, close to the convergence limit a VLLE algorithm is prompt to fail due to convergence to a trivial solution. This region constitutes a good area to test the robustness of a VLLE algorithm. The algorithm proposed in this work handled this region quite well. A closer look at the enlargements around the bicritical points shows that the convergence limit for the feasible region is very close to the three-phase boundary in the neighborhood of a few thousands in the mole fraction of CO₂.

In Figures 8–11, the phase behavior along pressure trajectories across the three phase envelop for constant CO₂ global mole fraction are presented. We have selected two CO₂ compositions for the Oil B system close to the bicritical point, one to the left at 99% mole (see Figures 8 and 9) and one to the right at 99.45% mol. in the retrograde zone (see Figures 10 and 11). The smooth change shown in Figures 8 and 9, even when the system crosses the phase boundaries is the typical behavior encountered in VLLE. In Figure 9 is appreciated how the vapor V and the CO₂-rich liquid L_2 approach each other in composition as the convergence limit is reached.

Figures 10 and 11 show the behavior in the retrograde region right to the bicritical point. In the increasing pressure trajectory, as one crosses the VLL-three-phase boundary, the

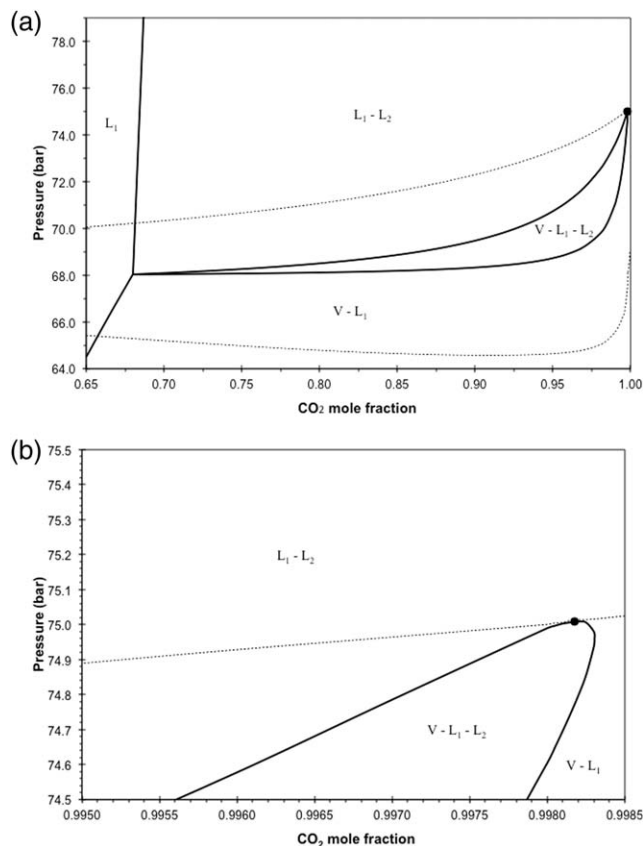


Figure 5. The phase diagram for CO₂ mixing with Malhamar Separator Oil at 305.35 K showing the phase regions.

V , L_1 , L_2 are the vapor, CO₂-lean, and CO₂-rich liquid phases. The solid lines are the phase boundaries and the dashed lines are the VLLE flash convergence limit. The solid circle represents the bicritical point. (a) Complete phase diagram and (b) enlargement around the CO₂-rich bicritical point.

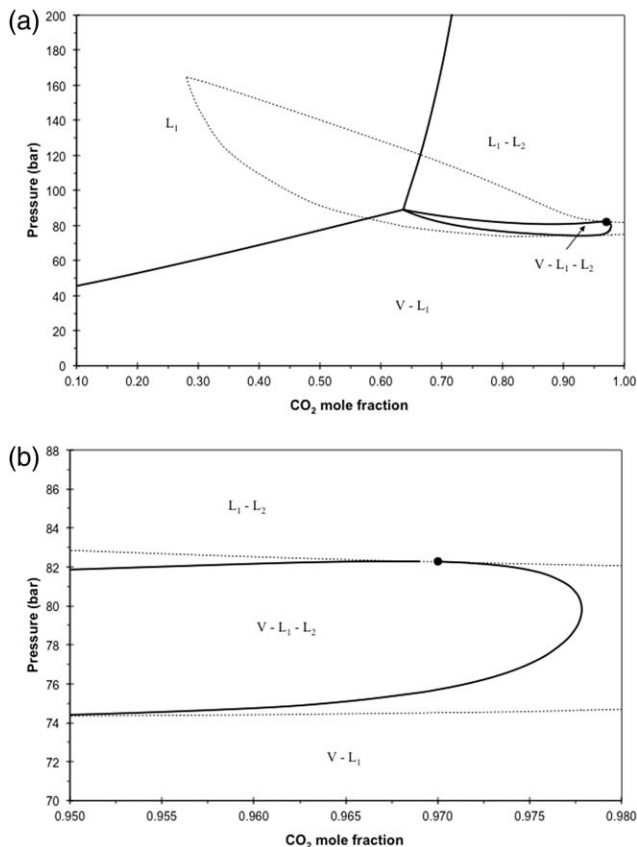


Figure 6. The phase diagram for CO₂ mixing with Bob Slaughter Block Oil at 313.71 K showing the phase regions.

V , L_1 , L_2 are the vapor, CO₂-lean, and CO₂-rich liquid phases. The solid lines are the phase boundaries and the dashed lines are the VLLE flash convergence limit. The solid circle represents the bicritical point. (a) Complete phase diagram and (b) enlargement around the CO₂-rich bicritical point.

CO₂-rich liquid L_2 appears as is the case left to the bicritical point trajectory (see Figure 8). As pressure is increased, the L_2 phase fraction increases as for a normal case, but it reaches a maximum and then falls down. As pressure is further increased, the L_2 phase disappears as the phase boundary is crossed at a higher pressure, contrary to the normal behavior. The CO₂ mole fractions of the three phases are reported in Figure 11. It is worth to mention that the difference in CO₂ mole fraction between the vapor V and CO₂-rich liquid L_2 is just a few thousandths, consequently, the properties of the two phases V and L_2 are very close to each other in the vicinity of the bicritical point. Left of the bicritical point in CO₂ composition, the system leaves the three-phase region and enters the two-phase region at the upper pressure phase boundary as CO₂-lean liquid L_1 and CO₂-rich liquid L_2 . Right of the bicritical point in CO₂ composition, the system leaves the three-phase region and enters the two-phase region at the upper pressure phase boundary as CO₂-lean liquid L_1 and vapor V . The label V or L_2 , for phases at pressures above the phase boundaries, is just a matter of convenience therefore, continuity is preserved.

As a final remark for these systems, we analyzed the SSI convergence for the outer loop. In Figure 12, we present the convergence evolution for phase fractions and in Figure 13 for

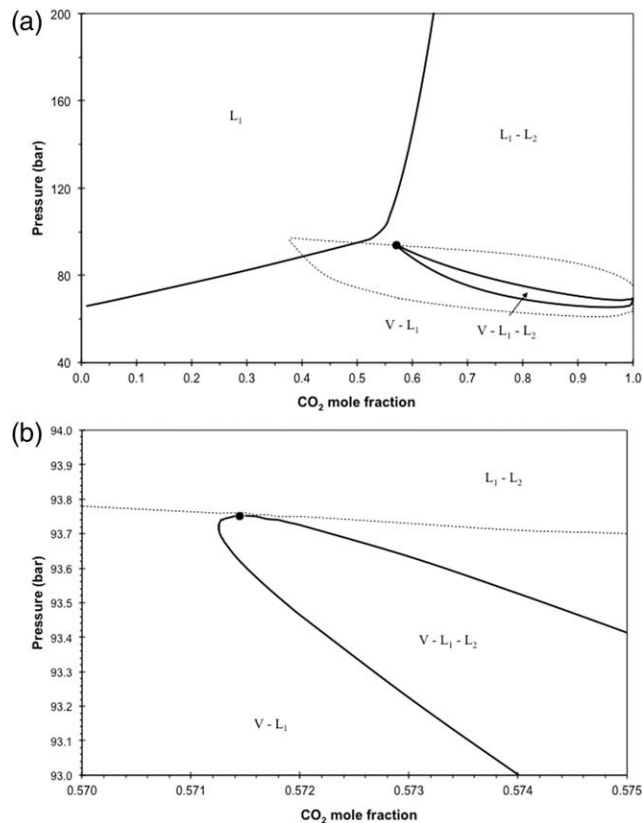


Figure 7. The phase diagram for CO₂ mixing with North Ward Estes Oil at 301.48 K showing the phase regions.

V , L_1 , L_2 are the vapor, CO₂-lean, and CO₂-rich liquid phases. The solid lines are the phase boundaries and the dashed lines are the VLLE flash convergence limit. The solid circle represents the bicritical point. (a) Complete phase diagram and (b) enlargement around the CO₂-lean bicritical point.

phase CO₂ mole fractions, for CO₂ mixing with Oil B to give 75% mol. of CO₂ at 307.6 K and 83.5 bar. This point calculation is typical of systems away from critical points. The

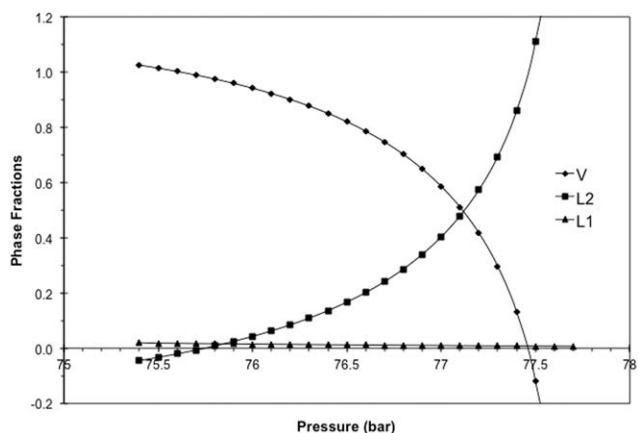


Figure 8. Phase fractions, vapor V (diamonds), CO₂-lean liquid L_1 (triangles), and CO₂-rich liquid L_2 (squares) for pressure trajectory across the three-phase envelop for CO₂ mixing with Oil B at 307.6 K.

The global CO₂ composition is held constant at 99% mol.

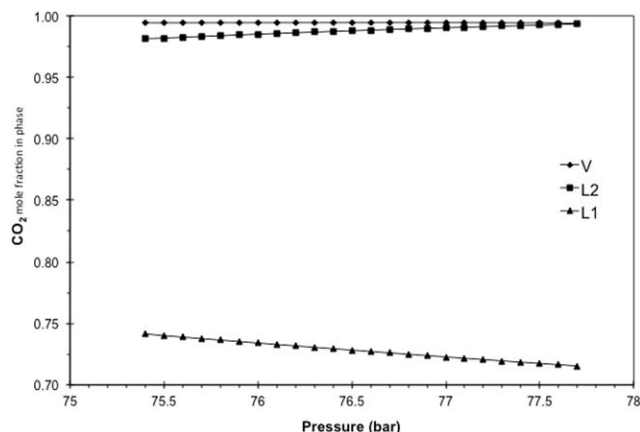


Figure 9. Phase CO₂ mole fraction, vapor V (diamonds), CO₂-lean liquid L₁ (triangles), and CO₂-rich liquid L₂ (squares) for pressure trajectory across the three-phase envelop for CO₂ mixing with Oil B at 307.6 K.

The global CO₂ composition is held constant at 99% mol.

convergence is stable and comes close to the solution after a few iterations.

In Figure 14, we present the convergence evolution for phase fractions and in Figure 15 for phase CO₂ mole fractions, for CO₂ mixing with Oil B to give 99.3% mol. of CO₂ at 307.6 K and 72 bar. This point calculation is typical of systems that are close to critical points. The convergence becomes more erratic and it takes longer to arrive close to the solution.

The initial estimates in Step 2 of Solution Procedure Section requires the election of a component as an almost a pure component for the second liquid phase composition estimate. For the cases studied in this work, the CO₂ was chosen as the almost pure component. At selected points, all other components were tested. The result was that the algorithm never converged when other component besides CO₂ was chosen. In almost all the tests, the initial equilibrium constants did not yield a solution for the inner loop.

A further test of the algorithm proposed was performed using the PEMEX Gas Condensate A fluid enriched with CO₂. The original fluid composition before the addition of CO₂ is presented in Table 1, along with the critical properties and nonzero temperature dependent binary interaction parameters. At a given temperature, the binary interaction parameters are calculated with the following expression

$$k_{ij} = k_{ij}^0 + \left(\frac{T}{1000} \right) k_{ij}^1 \quad (18)$$

In Figure 16, we present the phase diagram of the original fluid with the experimental data that was used to obtain the nonzero binary interaction parameters. It shows a narrow VLLE region at low temperatures and pressures. The original fluid was mixed with CO₂ to give a 16% mol. of CO₂. This system was analyzed and the resulting phase diagram is shown in Figure 17. This system shows regions of two and three liquid phases in equilibrium. That is, besides the one- and two-phase regions, it has regions of three phases: VLL and LLL, and a four phase region: VLLL. A thorough search covering the whole P-T plane was conducted to test the performance of

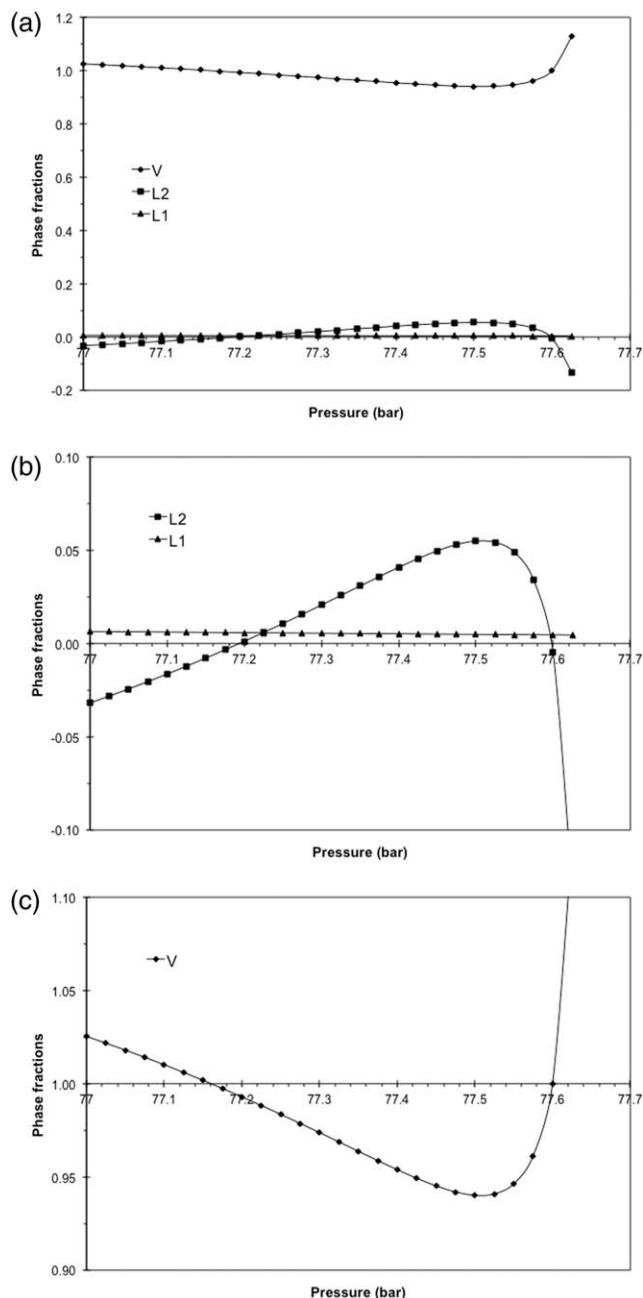


Figure 10. Phase fractions, vapor V (diamonds), CO₂-lean liquid L₁ (triangles), and CO₂-rich liquid L₂ (squares) for pressure trajectory across the three-phase envelop for CO₂ mixing with Oil B at 307.6 K.

The global CO₂ composition is held constant at 99.45% mol. (a) The three phases are shown, (b) enlargement for the two liquids L₁ and L₂, and (c) enlargement for the vapor V.

the VLLE flash algorithm. The results of the VLLE algorithm proposed in this article also served to construct the phase diagram. The procedure for the test was the following:

1. Perform calculations for the VLLE flash for a pressure vector at a given temperature. Select all the components as key components. If more than one solution is found, keep the ones that are different.

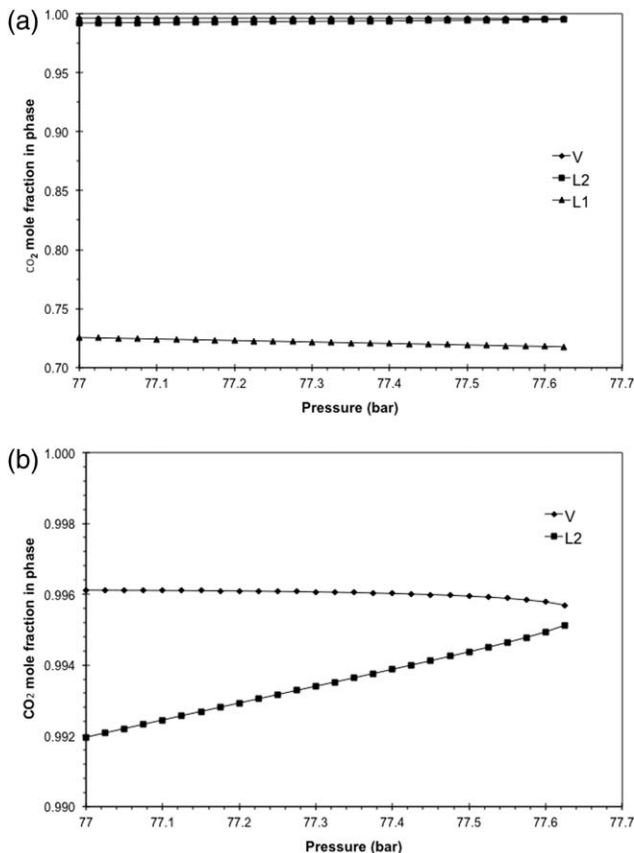


Figure 11. Phase CO_2 mole fraction, vapor V (diamonds), CO_2 -lean liquid L_1 (triangles), and CO_2 -rich liquid L_2 (squares) for pressure trajectory across the three-phase envelop for CO_2 mixing with Oil B at 307.6 K.

The global CO_2 composition is held constant at 99.45% mol. (a) The three phases are shown and (b) enlargement for vapor V and CO_2 -rich liquid L_2 .

2. Locate the VLL phase boundaries whenever a phase fraction is equal to zero. Interpolation between solutions may be necessary.

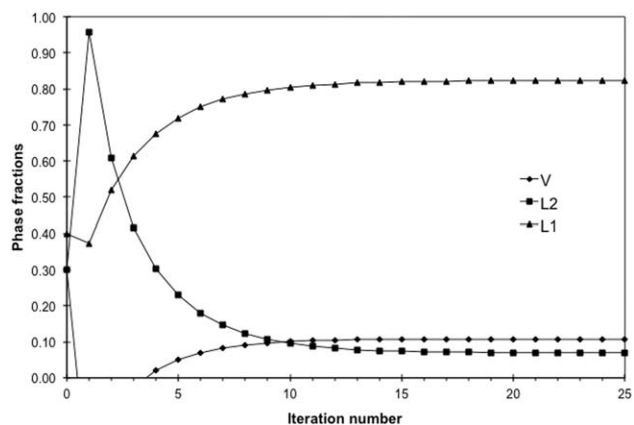


Figure 12. Convergence evolution in the outer loop for phase fractions, vapor V (diamonds), CO_2 -lean liquid L_1 (triangles), and CO_2 -rich liquid L_2 (squares) for CO_2 mixing with Oil B to give 75% mol. of CO_2 at 307.6 K and 83.5 bar.

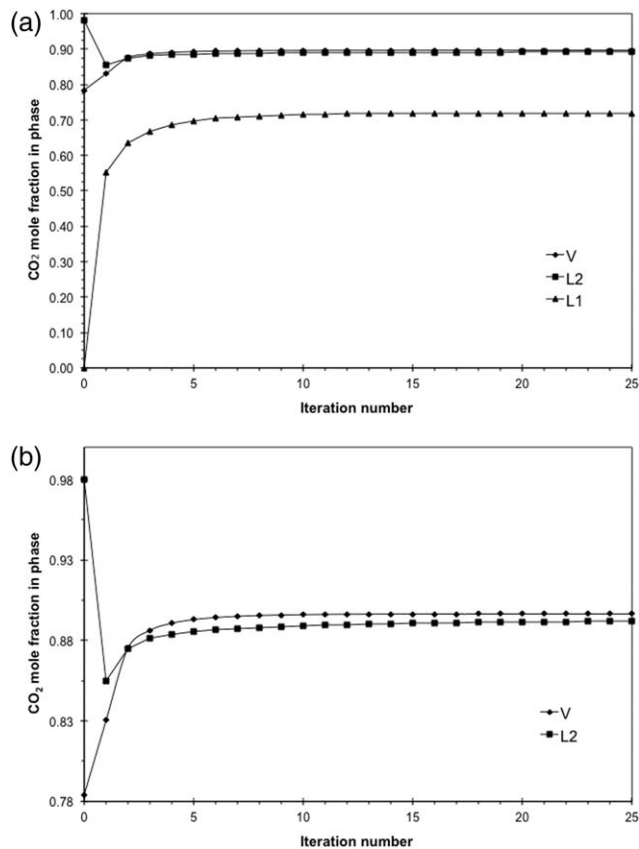


Figure 13. Convergence evolution in the outer loop for phase CO_2 mole fractions, vapor V (diamonds), CO_2 -lean liquid L_1 (triangles), and CO_2 -rich liquid L_2 (squares) for CO_2 mixing with Oil B to give 75% mol. of CO_2 at 307.6 K and 83.5 bar.

(a) The three phases are shown and (b) enlargement for vapor V and CO_2 -rich liquid L_2 .

3. Repeat the two previous steps for a temperature vector at a given pressure.

The general results of the test are: (a) solutions were found only when CO_2 , CH_4 , or N_2 were selected as key components.

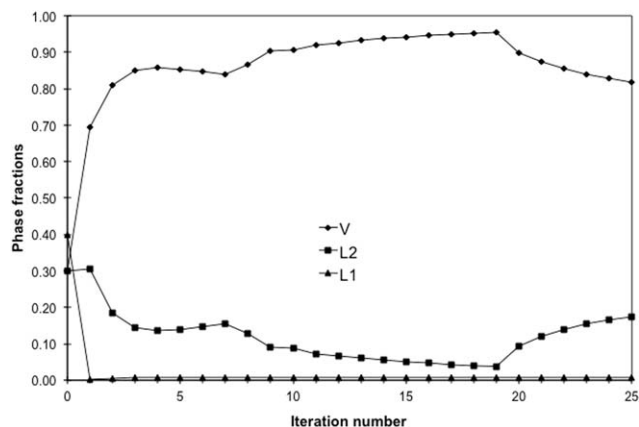


Figure 14. Convergence evolution in the outer loop for phase fractions, vapor V (diamonds), CO_2 -lean liquid L_1 (triangles), and CO_2 -rich liquid L_2 (squares) for CO_2 mixing with Oil B to give 99.3% mol. of CO_2 at 307.6 K and 77.2 bar.

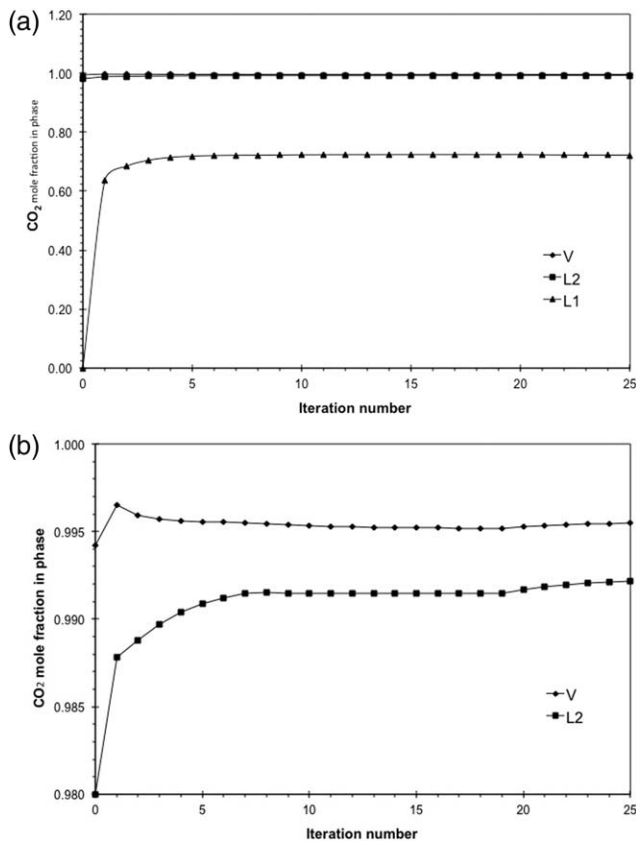


Figure 15. Convergence evolution in the outer loop for phase CO₂ mole fractions, vapor V (diamonds), CO₂-lean liquid L₁ (triangles), and CO₂-rich liquid L₂ (squares) for CO₂ mixing with Oil B to give 99.3% mol. of CO₂ at 307.6 K and 77.2 bar.

(a) The three phases are shown and (b) enlargement for vapor V and CO₂-rich liquid L₂.

In cases when a solution is found with N₂ as the key component, it was identical to the solutions found with CO₂ or CH₄. (b) In the VLL three-phase regions, the solutions were physically feasible with positive phase fractions. As the four-phase VLLL region was approached, the VLLE algorithm found two physically feasible solutions, one with CO₂ and the other with CH₄ as the key component. We retained the solution based on

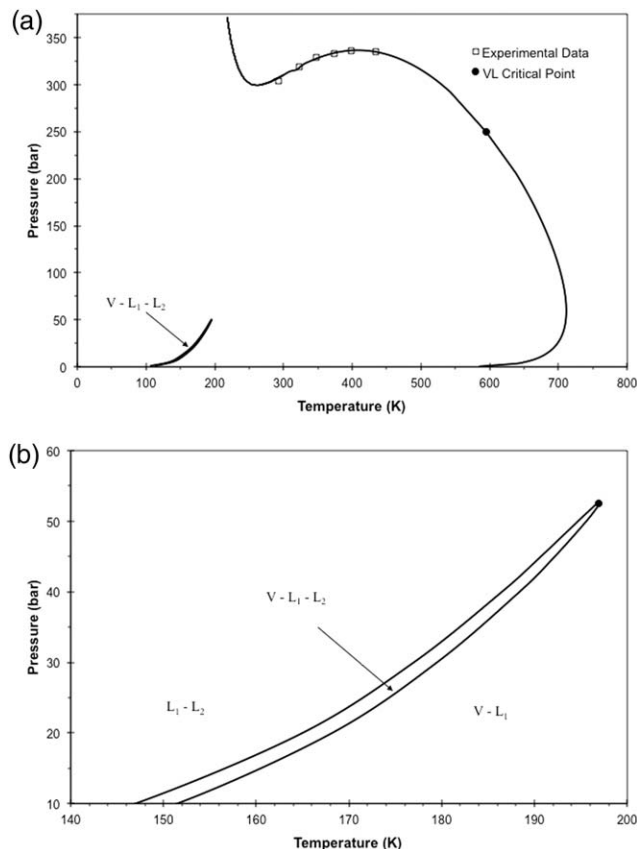


Figure 16. The phase diagram for PEMEX Gas Condensate A showing the phase regions.

V, L₁, L₂ are the vapor, heavy hydrocarbons-rich, and CO₂-rich liquid phases. The solid lines are the phase boundaries and the open squares are experimental data. (a) Complete phase diagram. The solid circle represents the VL critical point. (b) Enlargement around the VLL phase region. The solid circle represents the bicritical point.

the minimum Gibbs energy criteria. (c) The liquid phases found in the physically feasible solutions were labeled as follows: L₁ as the heavy hydrocarbon components (PC1 through PC5) rich liquid phase; L₂ as the CO₂-rich liquid phase; and L₃ as the CH₄-rich liquid phase. (d) In the V-L₁-L₂ region, the solution was always the one found with CO₂ as the key component. (e) In the V-L₁-L₃ region, the solution was always the

Table 1. Composition, Critical Properties, and Binary Interaction Coefficients for the PEMEX Gas Condensate A

Component	<i>n</i> (initial)	T _c (K)	P _c (bar)	ω	$k_{i,C1}^0$	$k_{i,C1}^1$	k_{i,CO_2}
N ₂	0.017620	126.20	34.00	0.0373			-0.017
CO ₂	0.009530	304.21	73.83	0.2236			
H ₂ S	0.001380	373.53	89.63	0.0942			0.0974
C1	0.615960	190.56	45.99	0.0115			0.0919
C2	0.056020	305.32	48.72	0.0995			0.1322
C3	0.026280	369.83	42.48	0.1523			0.1241
<i>i</i> C4	0.003890	407.80	36.40	0.1835			0.1200
<i>n</i> C4	0.014010	425.12	37.96	0.2002			0.1333
<i>i</i> C5	0.005400	460.40	33.80	0.2279			0.1219
<i>n</i> C5	0.007400	469.70	33.70	0.2515			0.1222
C6	0.027930	519.73	30.50	0.2987			0.1200
PC1	0.041020	563.595	30.527	0.3396	0.14205	-0.36513	0.1200
PC2	0.069796	632.811	24.921	0.4540	0.14205	-0.36513	0.1200
PC3	0.060786	724.857	17.962	0.6635	0.14205	-0.36513	0.1200
PC4	0.032821	820.911	12.419	0.9533	0.14205	-0.36513	0.1200
PC5	0.010158	916.547	8.592	1.3164	0.14205	-0.36513	0.1200

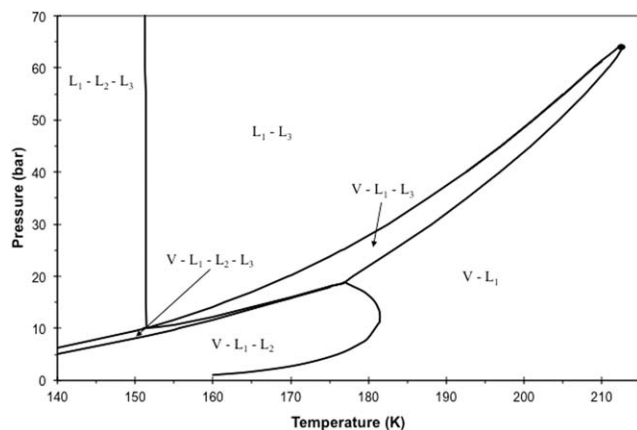


Figure 17. The phase diagram for CO₂ mixing with PEMEX Gas Condensate A showing the phase regions.

The global CO₂ composition is held constant at 16% mol. *V*, *L*₁, *L*₂, *L*₃ are the vapor, heavy hydrocarbons-rich, CO₂-rich, and CH₄-rich liquid phases. The solid lines are the phase boundaries. The solid circle represents the bicritical point.

one encountered with CH₄ as the key component. (f) At high pressures and low temperatures, three phases were found with positive phase fractions. The vapor phase has a liquid like density, therefore, the solution can be labeled as a LLL.

As examples of the phase behavior encountered, two trajectories were analyzed, one at 155 K and other at 30 bar. In Figure 18, phase fractions at 155 K are depicted as function of pressure for the solutions with CO₂ or CH₄ as the key components. At pressures below 9.5 bar and above 12.04 bar, the two solutions are identical. Between 9.5 and 12.04 bar, two different solutions were found. In the interval from 9.5 to 10.07 bar, the solution found with CO₂ as the key component has a lower Gibbs energy. In the interval from 10.07 to 12.04 bar, the solution found with CH₄ as the key component has a lower Gibbs energy. The solution with the greater Gibbs energy is shown with dotted lines. The phase boundary *V*-*L*₁-*L*₃ to *L*₁-*L*₃ is found when *V* = 0 at 11.67 bar when the CH₄ is the key component. The four-phase VLLL boundary is found with an

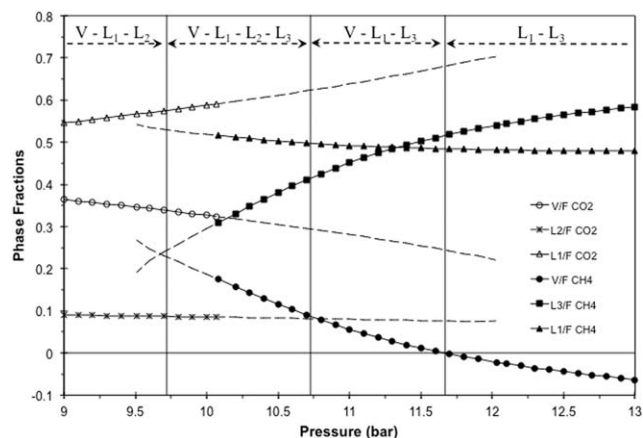


Figure 18. Phase fractions, vapor *V* (circles), heavy hydrocarbons-rich liquid *L*₁ (triangles), CO₂-rich liquid *L*₂ (asterisks), CH₄-rich liquid *L*₃ (squares) for pressure trajectory across the phase diagram for CO₂ mixing with PEMEX Gas Condensate A at 155 K.

The global CO₂ composition is held constant at 16% mol. Hollow symbols are for solutions with CO₂ key component and full symbols are for CH₄ key component. The continuation dotted lines are for solutions with a higher Gibbs energy. The phase boundaries are marked with vertical lines.

incipient phase search that does not alter the VLE algorithm. We introduce a fourth phase with zero phase fraction so that the VLLE equations are not modified. The initial estimate for the composition is based again on the key component concept. As initialization procedure for the fourth phase, a second key component is proposed, different from the one used in the VLLE calculation. For the Gas and Condensate A studied, the second key component was CH₄ or CO₂ depending on which component was selected in the VLLE calculation. Then, calculate fugacity coefficients and equilibrium constants as

$$K_{\text{new } i} = \frac{\phi_i^{L_1}}{\phi_i^{L_{\text{new}}}} \quad i = 1, \dots, n \quad (19)$$

Table 2. Component Phase Mole Fractions for the Phase Boundaries in the Pressure Trajectory at 155 K for the CO₂ Mixing with PEMEX Gas Condensate A

Component	9.72 bar				10.73 bar				11.67 bar			
	<i>V</i>	<i>L</i> ₁	<i>L</i> ₂	<i>L</i> ₃	<i>V</i>	<i>L</i> ₁	<i>L</i> ₂	<i>L</i> ₃	<i>V</i>	<i>L</i> ₁	<i>L</i> ₂	<i>L</i> ₃
N ₂	0.03917	0.00281	0.00108	0.00412	0.08479	0.00661	0.00263	0.01033	0.13453	0.01131	–	0.01840
CO ₂	0.01365	0.13940	0.86402	0.22133	0.01272	0.13641	0.85662	0.21899	0.01145	0.12824	–	0.18977
H ₂ S	0.00001	0.00191	0.00078	0.00121	0.00001	0.00159	0.00066	0.00091	0.00001	0.00154	–	0.00082
C1	0.94534	0.33386	0.12570	0.63660	0.90119	0.33166	0.13343	0.67150	0.85286	0.33334	–	0.69999
C2	0.00178	0.08065	0.00614	0.06008	0.00126	0.05984	0.00473	0.04241	0.00112	0.05594	–	0.03958
C3	0.00004	0.03851	0.00154	0.02525	0.00003	0.02974	0.00125	0.01802	0.00003	0.02818	–	0.01675
<i>i</i> C4	0.00000	0.00572	0.00009	0.00355	0.00000	0.00450	0.00007	0.00255	0.00000	0.00427	–	0.00239
<i>n</i> C4	0.00000	0.02061	0.00035	0.01163	0.00000	0.01678	0.00031	0.00850	0.00000	0.01611	–	0.00791
<i>i</i> C5	0.00000	0.00796	0.00005	0.00420	0.00000	0.00661	0.00005	0.00310	0.00000	0.00637	–	0.00290
<i>n</i> C5	0.00000	0.01090	0.00007	0.00541	0.00000	0.00925	0.00006	0.00403	0.00000	0.00896	–	0.00375
C6	0.00000	0.04118	0.00009	0.01744	0.00000	0.03660	0.00009	0.01319	0.00000	0.03582	–	0.01229
PC1	0.00000	0.06049	0.00009	0.00477	0.00000	0.06696	0.00010	0.00356	0.00000	0.06855	–	0.00308
PC2	0.00000	0.10295	0.00001	0.00366	0.00000	0.11691	0.00001	0.00249	0.00000	0.12002	–	0.00206
PC3	0.00000	0.08966	0.00000	0.00072	0.00000	0.10329	0.00000	0.00040	0.00000	0.10610	–	0.00032
PC4	0.00000	0.04841	0.00000	0.00004	0.00000	0.05594	0.00000	0.00002	0.00000	0.05746	–	0.00001
PC5	0.00000	0.01498	0.00000	0.00000	0.00000	0.01732	0.00000	0.00000	0.00000	0.01779	–	0.00000
Phase Fractions	0.3380	0.5750	0.0871	0.0000	0.0868	0.4975	0.0000	0.4157	–0.0002	0.4843	–	0.5159

The global CO₂ composition is held constant at 16% mol. Vapor *V*, heavy hydrocarbons-rich liquid *L*₁, CO₂-rich liquid *L*₂, CH₄-rich liquid *L*₃.

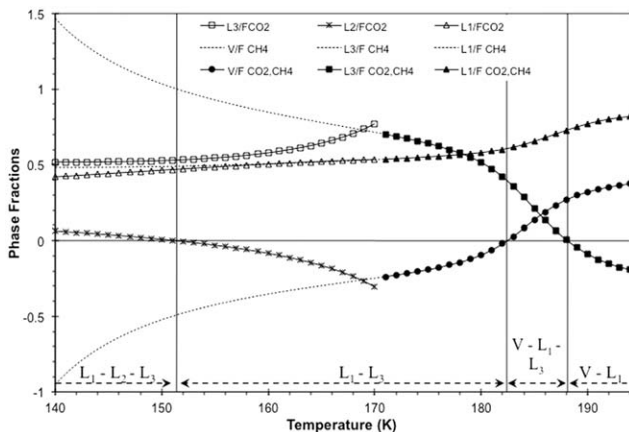


Figure 19. Phase fractions, vapor V (circles), heavy hydrocarbons-rich liquid L_1 (triangles), CO_2 -rich liquid L_2 (asterisks), CH_4 -rich liquid L_3 (squares) for temperature trajectory across the phase diagram for CO_2 mixing with PEMEX Gas Condensate A at 30 bar K.

The global CO_2 composition is held constant at 16% mol. Hollow symbols are for solutions with CO_2 key component and full symbols are for either CO_2 or CH_4 key component. The continuation dotted lines are for solutions with CH_4 key component. The phase boundaries are marked with vertical lines.

In the outer loop of the VLLE algorithm, we generate a new estimate for the composition of the fourth phase

$$u_i = K_{\text{new}i} x_i \quad i = 1, \dots, n \quad (20)$$

Then, calculate the summation of the mole fractions of the fourth phase and normalize the mole fractions with

$$S_u = \sum_{i=1}^n u_i \quad (21)$$

Finally, calculate the following error function to verify the equilibrium conditions

$$\text{Error} = \sum_{i=1}^n |x_i \phi_i^{L_1} - u_i \phi_i^{L_{\text{new}}}| \quad (22)$$

As the VLLE flash approaches convergence, the summation S_u and error function Error approach limiting values. The fourth phase will be in equilibrium with the other three phases at a given temperature and pressure when the summation S_u is equal to unity and the error function Error approaches zero within a tolerance.

At 155 K, the transition to the four phase region was found at 9.72 bar when the key component was CO_2 in the VLLE flash and CH_4 in the fourth phase; and at 10.73 bar, when the key component was CH_4 in the VLLE flash and CO_2 in the fourth phase. In Table 2, we report the compositions at equilibrium for the pressures of the phase transitions for the trajectory at 155 K. Note the distinct phase component mole fractions for all the phases. The summation S_u had values greater than 1 inside the four phase region and less than 1 outside this region.

In Figure 19, the phase fractions at 30 bar are depicted as function of temperature for the solutions with CO_2 or CH_4 as the key component. For the CO_2 solution, the vapor phase adopted a liquid like density for temperatures lower than 170.5 K, so it was labeled as liquid. At temperatures above 170.5 K, the two solutions are identical. For temperatures below 170.5 K, two different solutions were found. For temperatures below 151 K, the solution with CO_2 has positive phase fractions and the solution with CH_4 the vapor has a negative phase fraction; therefore, the solution for CO_2 is the correct one. The phase boundary $V-L_1-L_3$ to $V-L_1$ is found when $L_3 = 0$ at 188.1 K when either CH_4 or CO_2 is selected as the key component. The phase boundary $V-L_1-L_3$ to L_1-L_3 is found when $V = 0$ at 182.4 K when CH_4 or CO_2 is the key component. The phase boundary $L_1-L_2-L_3$ to L_1-L_2 is found when $L_3 = 0$ at 151.4 K when CO_2 is the key component. In Table 3, we report the compositions at equilibrium for the temperatures of the phase transitions for the trajectory at 30 bar. Note the distinct phase component mole fractions for all the phases.

The general findings based on the results of the six systems studied in this work, are the following:

Table 3. Component Phase Mole Fractions for the Phase Boundaries in the Temperature Trajectory at 30 bar for the CO_2 Mixing with PEMEX Gas Condensate A

Component	151.38 K				182.44 K				188.09 K			
	V	L_1	L_2	L_3	V	L_1	L_2	L_3	V	L_1	L_2	L_3
N_2	–	0.01143	0.00413	0.01805	0.08533	0.01118	–	0.02119	0.04129	0.00515	–	0.00827
CO_2	–	0.12355	0.86989	0.19233	0.03300	0.15088	–	0.17308	0.05078	0.20070	–	0.27134
H_2S	–	0.00154	0.00061	0.00085	0.00004	0.00148	–	0.00069	0.00006	0.00158	–	0.00095
C1	–	0.32549	0.12036	0.69645	0.87722	0.39153	–	0.72509	0.90135	0.38177	–	0.61017
C2	–	0.05626	0.00365	0.03976	0.00412	0.05369	–	0.03775	0.00608	0.06289	–	0.04743
C3	–	0.02826	0.00092	0.01701	0.00025	0.02718	–	0.01466	0.00039	0.03042	–	0.01920
$i\text{C}_4$	–	0.00428	0.00005	0.00243	0.00001	0.00413	–	0.00201	0.00002	0.00452	–	0.00263
$n\text{C}_4$	–	0.01614	0.00021	0.00811	0.00002	0.01543	–	0.00637	0.00003	0.01628	–	0.00848
$i\text{C}_5$	–	0.00638	0.00003	0.00298	0.00000	0.00609	–	0.00223	0.00000	0.00628	–	0.00298
$n\text{C}_5$	–	0.00898	0.00004	0.00388	0.00000	0.00852	–	0.00280	0.00000	0.00860	–	0.00380
C6	–	0.03593	0.00005	0.01286	0.00000	0.03361	–	0.00834	0.00000	0.03247	–	0.01167
PC1	–	0.07072	0.00006	0.00301	0.00000	0.05531	–	0.00314	0.00000	0.04767	–	0.00606
PC2	–	0.12388	0.00001	0.00198	0.00000	0.09615	–	0.00223	0.00000	0.08111	–	0.00538
PC3	–	0.10951	0.00000	0.00029	0.00000	0.08473	–	0.00042	0.00000	0.07063	–	0.00149
PC4	–	0.05929	0.00000	0.00001	0.00000	0.04588	–	0.00003	0.00000	0.03814	–	0.00016
PC5	–	0.01835	0.00000	0.00000	0.00000	0.01421	–	0.00000	0.00000	0.01180	–	0.00001
Phase Fractions	–	0.4693	–0.0001	0.5307	–0.0027	0.6065	–	0.3963	0.2710	0.7299	–	–0.0009

The global CO_2 composition is held constant at 16% mol. Vapor V, heavy hydrocarbons-rich liquid L_1 , CO_2 -rich liquid L_2 , CH_4 -rich liquid L_3 .

1. If only one solution is found with positive phase fractions, it corresponds to a valid VLLE solution.

2. If more than one solution is found with positive phase fractions, the minimum Gibbs energy criteria is used to select a solution. A fourth phase is proposed and tested using the S_u summation. If $S_u < 1$, the system is in a VLLE region and the solution is valid. If $S_u > 1$, the system is in a VLLLE region and the solution is not valid, consequently a further VLLLE flash must be solved.

3. If a negative VLLE flash solution is found or no solution is found at all, the system lies in a region with two phases at most. The equilibrium solution must be found by the appropriate two phase flash.

Concluding Remarks

The algorithm proposed in this work for the solution of a stand-alone three-phase VLL equilibrium flash calculation is stable and robust. The inverse barrier function to solve for the phase fractions in the inner loop always warrants arriving to the solution whenever it exists. This methodology is easy to implement in any algorithm that solves the RR equations. The SSI in the outer loop has a slow rate of convergence, nevertheless it is a good method as a starting point for a higher order method, even close to critical points. The challenging cases analyzed showed that the initialization procedure proposed in this work is a good starting point for a stable three-phase VLLE flash algorithm. The key component concept is robust and allowed to generate the liquid phases present in equilibrium at the different three-phase regions. For the CH₄ and CO₂ rich mixture of the Gas and Condensate A fluid, the Gibbs energy criteria helped to determine the valid solution when two physically feasible solutions were found. A simple extension was presented to calculate the VLLL phase boundary when a third liquid phase was present.

The results found for the negative flash in the region outside the three-phase physical domain are continuous; therefore, it allowed us to calculate the VLL phase boundaries.

Acknowledgment

The authors acknowledge the invitation to contribute to this homage to Prof. John M. Prausnitz, an outstanding professor for many of us that learned to love thermodynamics with him.

Notation

B = augmented inverse barrier function
 B_{wx}, B_{yx} = augmented inverse barrier function residuals
 E = inequality material balance equation
Error = Error function for the fourth phase
 f = fugacity
 K_1 = vapor to first liquid equilibrium constant
 K_2 = second liquid to first liquid equilibrium constant
 K_{new} = fourth phase to first liquid equilibrium constant
 n = number of components
 Q = objective function for minimization
 r = barrier parameter
 RR_{wx}, RR_{yx} = Rachford-Rice residuals
 u = fourth-phase mole fraction
 w = second liquid mole fraction
 x = first liquid mole fraction
 y = vapor mole fraction
 z = global mole fraction
 β_1, β_2 = vapor and second liquid phase fractions

ϕ = fugacity coefficient
 θ = phase fractions vector

Subscripts

i = component
 wx = second minus first liquid
 yx = vapor minus first liquid

Superscripts

V = vapor phase label
 L_1 = first liquid phase label
 L_2 = second liquid phase label
 L_3 = third liquid phase label

Literature Cited

- Whitson CH, Michelsen ML. The negative flash. *Fluid Phase Equilib.* 1989;53:51–71.
- Iranshahr A, Voskov D, Tchepeli HA. Generalized negative-flash method for multiphase multicomponent systems. *Fluid Phase Equilib.* 2010;299:272–284.
- Leibovici CF, Neoschil J. A solution of Rachford-Rice equations for multiphase systems. *Fluid Phase Equilib.* 1995;112:217–221.
- Haugen KB, Firoozabadi A, Sun L. Efficient and robust three-phase split computations. *AIChE J.* 2011;57(9):2555–2565.
- Li Z, Firoozabadi A. General strategy for stability testing and phase-split calculation in two and three phases. *SPE J.* 2012;17(4):1096–1107.
- Li Z, Firoozabadi A. Initialization of phase fractions in Rachford-Rice equations for robust and efficient three-phase split calculation. *Fluid Phase Equilib.* 2012;332:21–27.
- Okuno R, Johns RT, Sepahmooli K. A new algorithm for Rachford-Rice for multiphase compositional simulation. *SPE J.* 2010;15(2):313–325.
- Yan W, Stenby EH. On solving the Rachford-Rice equation with higher order methods. *Fluid Phase Equilib.* 2014;363:290–292.
- Michelsen ML. Calculation of multiphase equilibrium. *Comput Chem Eng.* 1994;18(7):545–550.
- Leibovici CF, Nichita DV. A new look at multiphase Rachford-Rice equations for negative flashes. *Fluid Phase Equilib.* 2008;267:127–132.
- Lucia A, Padmanabhan L, Venkataraman S. Multiphase equilibrium flash calculations. *Comput Chem Eng.* 2000;24:2557–2569.
- Bausa J, Marquardt W. Quick and reliable phase stability test in VLLE flash calculations by homotopy continuation. *Comput Chem Eng.* 2000;24:2447–2456.
- Saber N, Shaw JM. Rapid and robust phase behavior stability analysis using global optimization. *Fluid Phase Equilib.* 2008;264:137–146.
- Jalali F, Seader JD, Khaleghi S. Global solution approaches in equilibrium and stability analysis using homotopy continuation in the complex domain. *Comput Chem Eng.* 2008;32:2333–2345.
- Nichita DV, Gomez S. Efficient location of multiple global minima for the phase stability problem. *Chem Eng J.* 2009;152:251–263.
- Petitfrere M, Nichita DV. Robust and efficient trust-region based stability analysis and multiphase flash calculations. *Fluid Phase Equilib.* 2014;362:51–68.
- Treble MA. A preliminary evaluation of two and three phase flash initiation procedures. *Fluid Phase Equilib.* 1989;53:113–122.
- Bunz AP, Dohrn R, Prausnitz JM. Three-phase flash calculations for multicomponent systems. *Comput Chem Eng.* 1991;15(1):47–51.
- Prausnitz JM, Anderson TF, Grens EA, Eckert CA, Hsieh R, O'Connell JP. *Computer Calculations for Multicomponent Vapor-Liquid and Liquid-Liquid Equilibria*. New York: Prentice-Hall International, 1980.
- Garcia-Sanchez F, Schwartzenruber J, Ammar MN, Renon H. Modeling of multiphase equilibria for multicomponent mixtures. *Fluid Phase Equilib.* 1996;121:207–225.
- Peng DY, Robinson DB. A new two-constant equation of state. *Ind Eng Chem Fundam.* 1976;15(1):59–64.
- Luenberger DG, Ye Y. *Linear and Nonlinear Programming*, 3rd ed. New York: Springer Science + Business Media, LLC, 2008.
- Mathias PM, Boston JF, Watanasiri S. Effective utilization of equations of state for thermodynamic properties in process simulation. *AIChE J.* 1984;30:182–186.

Manuscript received Dec. 18, 2014, and revision received June 21, 2015.